

Accepted Manuscript

New thiobarbituric acid scaffold-based small molecules: Synthesis, cytotoxicity, 2D-QSAR, pharmacophore modelling and in-silico ADME screening

Heba S.A. El-Zahabi, Maha M.A. Khalifa, Yomna M.H. Gado, Amel M. Farrag, Mahmoud M. Elaasser, Nesreen A. Safwat, Reham R. AbdelRaouf, Reem K. Arafa



PII: S0928-0987(19)30027-2
DOI: <https://doi.org/10.1016/j.ejps.2019.01.023>
Reference: PHASCI 4814

To appear in: *European Journal of Pharmaceutical Sciences*

Received date: 7 December 2018
Revised date: 12 January 2019
Accepted date: 18 January 2019

Please cite this article as: H.S.A. El-Zahabi, M.M.A. Khalifa, Y.M.H. Gado, et al., New thiobarbituric acid scaffold-based small molecules: Synthesis, cytotoxicity, 2D-QSAR, pharmacophore modelling and in-silico ADME screening, *European Journal of Pharmaceutical Sciences*, <https://doi.org/10.1016/j.ejps.2019.01.023>

This is a PDF file of an unedited manuscript that has been accepted for publication. As a service to our customers we are providing this early version of the manuscript. The manuscript will undergo copyediting, typesetting, and review of the resulting proof before it is published in its final form. Please note that during the production process errors may be discovered which could affect the content, and all legal disclaimers that apply to the journal pertain.

New Thiobarbituric Acid Scaffold-based Small Molecules: Synthesis, Cytotoxicity, 2D-QSAR, Pharmacophore Modeling and in-silico ADME Screening

Heba S.A. El-Zahabi^a, Maha M. A. Khalifa^a, Yomna M. H. Gado^a, Amel M. Farrag^a, Mahmoud M. Elaasser^b, Nesreen A. Safwat^b, Reham R. AbdelRaouf,^c Reem K. Arafa^{c,*}

^a Department of Pharmaceutical Chemistry, Faculty of Pharmacy, Al-Azhar University, Cairo 11884, Egypt.

^b The Regional Center for Mycology and Biotechnology, Al-Azhar University, Cairo, Egypt.

^c Biomedical Sciences Program, Zewail City of Science and Technology, 12578, Cairo, Egypt.

Abstract

A series of twenty five new thiobarbituric acid derivatives, *viz.* **3a-h**, **4-7**, **8a-c**, **9**, **10a-c**, **11** and **12a-d**, were designed and synthesized as potential cytotoxic agents. *In-vitro* screening of the new compounds against the three human cancer cell lines Caco-2, HepG-2 and MCF-7 was performed to assess their intrinsic activity. Compound **12d** exhibited potent sub-micromolar activity against HepG-2 and MCF-7 ($IC_{50} = 0.07$ and $0.08 \mu M$, respectively). *In-silico* pharmacophore modelling of this chemotype compounds disclosed a five features' pharmacophore model representing essential steric and electronic fingerprints essential for activity. Finally, a 2D-QSAR model was devised to quantitatively correlate the 2D molecular feature descriptors of this series of thiobarbiturates with their cytotoxic activity against MCF-7. Finally, *in silico* evaluation of the physicochemical and ADME properties of these derivatives was performed.

Key words: Thiobarbituric acid derivatives; Merbarone; cytotoxic activity; pharmacophore; 2D-QSAR.

*Corresponding author

Reem K. Arafa

Professor of Biomedical Sciences

University of Science and Technology

Zewail City of Science and Technology

Ahmed Zewail Road

October Gardens, 6th of October City, Giza, Egypt, 12578

Mobile: +2-01002074028

E-mail: rkhidr@zewailcity.edu.eg

1. Introduction

Thiobarbiturate scaffold based small molecules have been reported to possess antitumor capacity with the observed activity being attributed to targeting different enzymes having an important role in cancer development^[1-11] e.g. topoisomerase II^[1], sirtuins^[6-8, 10] and B-Raf protein kinase^[9].

National Cancer Institute (NCI/USA) reported the thiobarbiturate analogue Merbarone **I** as potent antitumor agent in fighting melanoma and sarcoma cancer via inhibiting topoisomerase II^[1, 4]. In addition, other thiobarbiturate derivatives e.g. **II**^[6], **III**^[10] and **IV**^[10] displayed remarkable activities against cancer cell lines via inhibiting Sirt1 and/or Sirt2 enzymes (**Figure 1**). Focusing on B-Raf kinase as a key enzyme that demonstrated mutations in a broad range of human cancers, B-Raf^{V600E} is considered an important target for anticancer drugs. Recently, novel thiobarbiturate derivatives **V** and **VI** were reported as B-Raf^{V600E} inhibitors (**Figure 1**)^[9].

In medicinal chemistry, the thiobarbiturate ring represents an excellent scaffold being incorporated in many biologically active small molecules, e.g. antitumor agents^[1-14], antivirals^[15-17] and antimicrobials^[18-21], in addition to the well-known clinically used CNS depressant thio/barbiturates. Structurally speaking, compounds **II-VI** chemotype can be envisaged as having two subdomains, a non-modified chemical moiety (domain **A**, thiobarbituric scaffold) and a C5 modifiable domain **B** with a methyldene bridge as a linker. Domain **B** is represented by aryl or heteroaryl groups (**Figure 1**).

Modification of moiety **B** was attributed to the replacement of the furfuryl nucleus in **V** and **VI** with aliphatic, aryl and heteroaryl groups. Compounds **4-6** and **9** included the replacement of furfuryl nucleus (moiety **B**) in **V** and **VI** with thiobarbituric acid motif using either aliphatic or aryl diamine linkers. Modification in compounds **2, 3 a-h, 7, 10 a-c, 11** and **12a-d**, represented replacement of **B** by (aryl/heteroaryl) groups. Simultaneously, various amines (amino group, hydrazone, hydrazinocarbonyl, hydrazinosulfone and thiosemicarbazide moieties) were applied as a linker. The last modification, displayed isosteric switching of furfuryl ring in **V** and **VI** to pyrazole ring in **8a-c**. (**Figure 2**).

Based on these findings and in line with our continuous investigation for anticancer agents with variable chemical scaffolds^[19-21], a new series of C5 substituted thiobarbiturates was designed and synthesized with a focus on maintaining the thiobarbituric scaffold and exchanging methyldene-bridge attached substituents at C5 of the thiobarbiturate ring. Biological assessment of the cytotoxic ability of these new compounds was performed against 3 human cancer cell lines, *viz.* Caco-2 (colorectal cancer), HepG-2 (liver cancer) and MCF-7 (breast cancer). Further, pharmacophore modelling was carried out to extract the important steric and electronic features of this class of compounds underlying their inherent pharmacological activity. Subsequently, a 2D-QSAR model based on the MCF-7 cytotoxicity data was built to quantitatively correlate 2D structural features descriptors with the observed cytotoxicity. Finally, in silico assessment of the physicochemical and ADME properties of all compounds was performed.

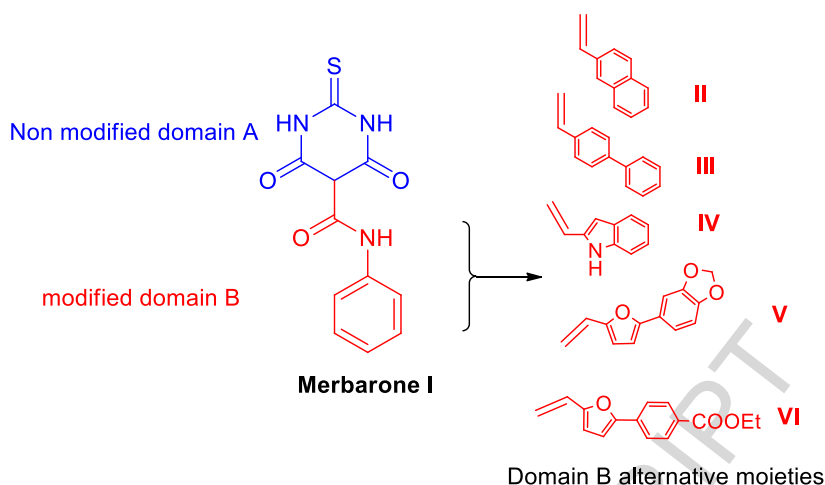


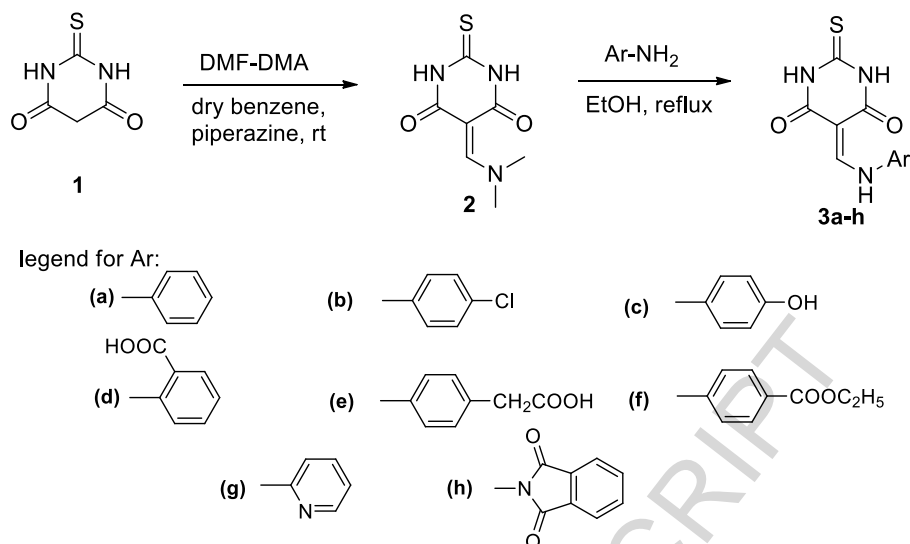
Figure 1: Merbarone I and thiobarbiturate analogues with promising anticancer activity

2. Result and discussion

2.1. Chemistry

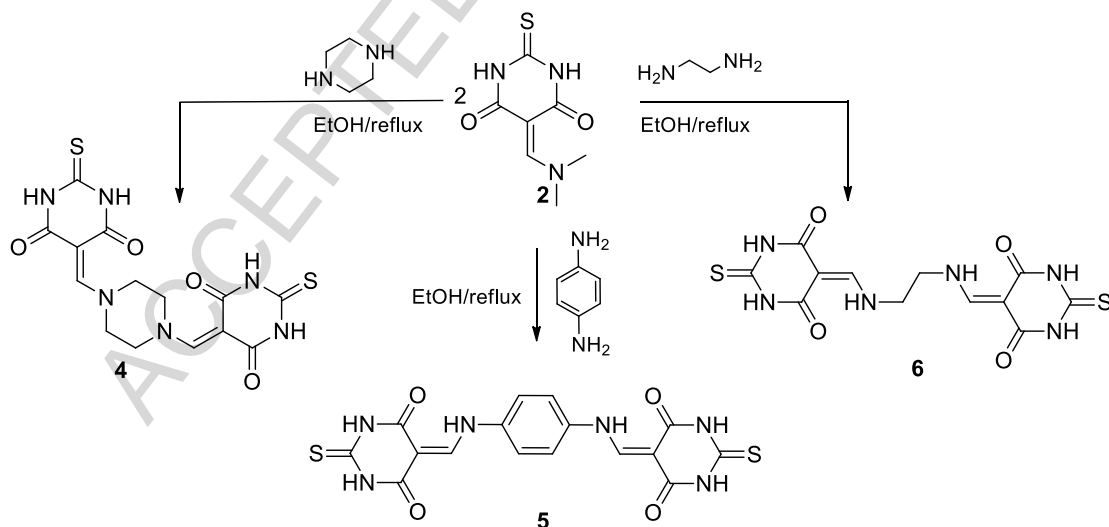
Synthesis of the target compounds is depicted in schemes 1-5. 5-[(Dimethylamino)methylidene]-2-thioxodihydropyrimidine-4,6(1*H*,3*H*)-dione (**2**) was prepared by reacting thiobarbituric acid **1** with *N,N'*-dimethylformamide dimethylacetal (DMF-DMA) in dry benzene, adopting the reported condition^[22,23] (**Scheme 1**). ¹H-NMR spectrum of **2** revealed the presence of two signals at δ 3.50 and 7.88 ppm for the protons corresponding to the di-CH₃ groups and vinylic (=CH-N) proton, respectively. The mass spectrum showed a molecular ion peak [M⁺] at *m/z*: 199. The IR chart displayed bands at 3102 and 1603 cm⁻¹ representing to the NH and CO groups, respectively.

Precursor **2** was reacted with different aromatic amines adopting the reported procedure^[24] to afford the corresponding dihydro-5-[(arylamino)methylidene]-2-thioxopyrimidine-4,6(1*H*,3*H*)-dione **3a-h** (**Scheme 1**). The proposed structures of **3a-h** were compatible with their elemental and spectral data where their ¹H-NMR spectra showed the disappearance of the singlet signal at δ 3.50 ppm for the protons of the di-CH₃ groups, in each case. Mass spectra of **3a-h** illustrated a peak for each expected molecular ion (Experimental section).



Scheme 1: Synthesis of derivatives **3a-h**.

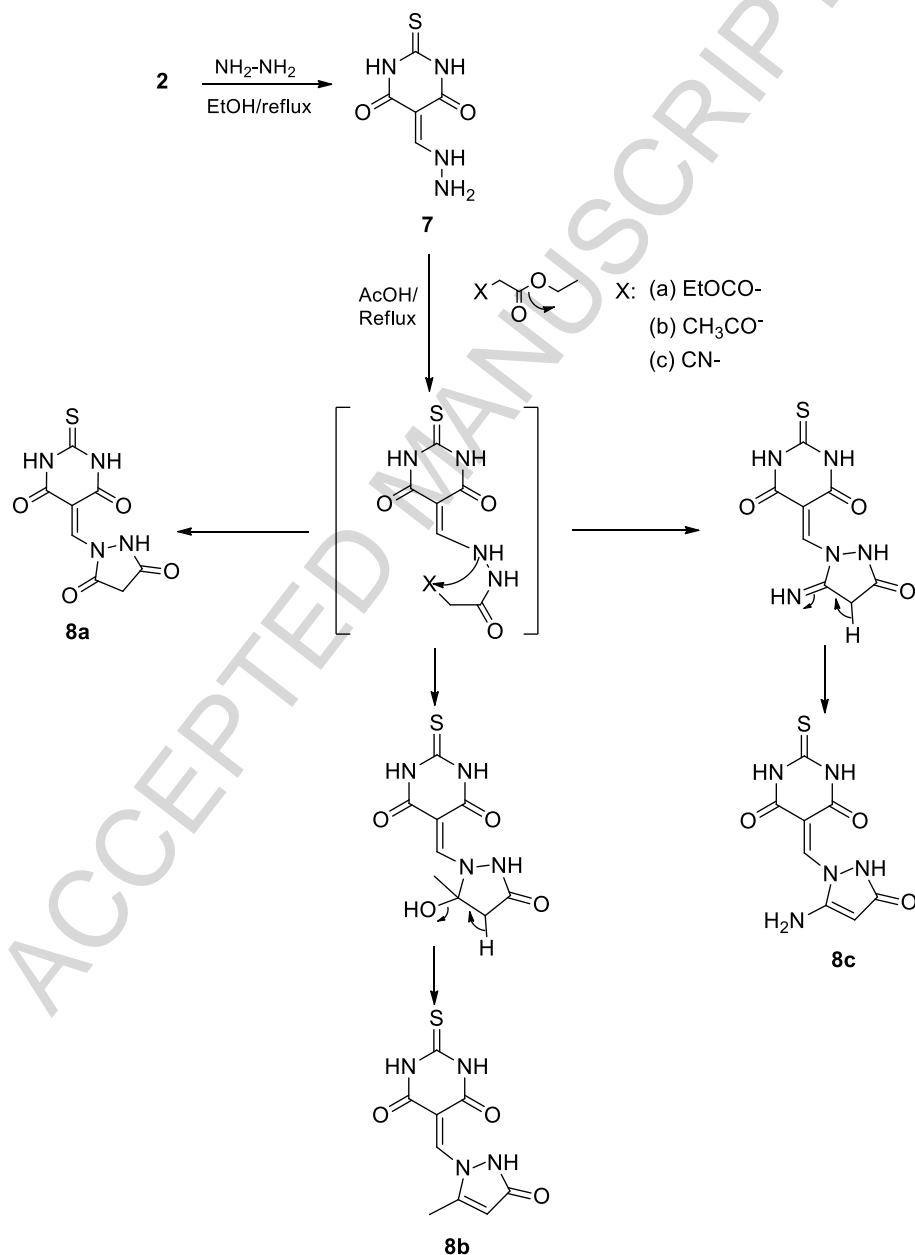
In a similar manner, precursor **2** was reacted with different diamines, *viz.* piperazine, 1,4-phenyldiamine and ethylenediamine, to afford bis[2-thioxo-dihydropyrimidine-4,6(1*H*,3*H*)-dione] derivatives **4-6** (**Scheme 2**). ¹H-NMR spectrum of *N,N*-bis[5-methylidene-2-thioxo-dihydropyrimidine-4,6(1*H*,3*H*)-dione]piperazine **4** revealed a multiplet signal at δ 3.07-3.09 ppm characterizing aliphatic protons of the piperazine ring. Concomitantly, ¹H-NMR spectrum of **5** revealed two doublets at δ 6.61 ppm and 7.16 ppm ($J = 8.7$ Hz) assigned to the aromatic ring protons and a signal appeared at δ 8.38 ppm for the vinylic proton (=CH-N).



Scheme 2: Synthesis of derivatives **4-6**.

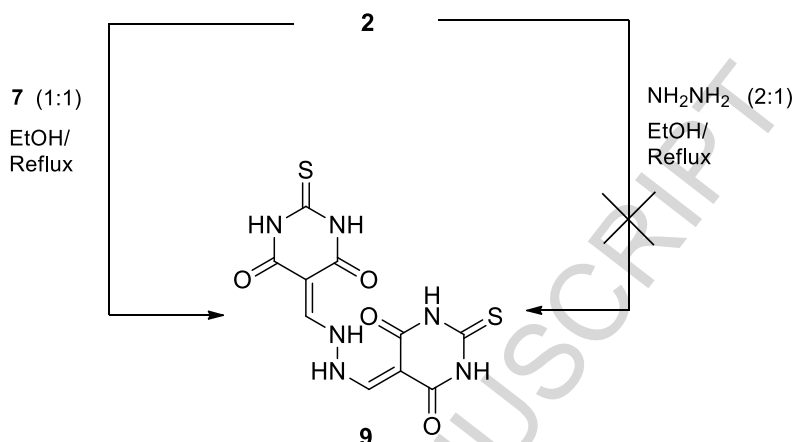
Upon reacting compound **2** with one mole equivalent ratio of hydrazine hydrate in refluxing ethanol, 5-(hydrazinylmethylidene)-2-thioxo-dihydropyrimidine-4,6(1*H*,3*H*)-dione **7** was afforded^[25,26]. Subsequently, reaction of **7** with diethylmalonate, ethyl acetoacetate or ethyl cyanoacetate was carried in acetic acid under reflux to afford the corresponding cycloaddition pyrazolyl products **8a-c**, respectively (**Scheme 3**). ¹H-NMR spectrum of **8a** revealed the appearance of

singlet at δ 2.89 ppm, integrated for two protons at C4 of the pyrazole ring. Mass spectrum illustrated a molecular ion peak $[M^+]$ at m/z 254. $^1\text{H-NMR}$ spectra of **8b** and **8c** exhibited a singlet at δ 5.63 ppm and 7.47 ppm corresponding for the vinylic proton at C4 of the pyrazole ring, respectively. Also, $^1\text{H-NMR}$ of **8b** revealed a signal at δ 2.22 ppm for the CH_3 group at C5 of the pyrazole ring, while **8c** expressed D_2O exchangeable singlet at δ 11.31 ppm for NH_2 protons. $^{13}\text{C-NMR}$ for **8b** showed a signal at 145.18 ppm representing the vinylic carbon and three signals at 158.00, 161.90 and 163.00 ppm representing three carbonyl carbons. Mass spectra of **8b** and **8c** showed molecular ion peaks $[M^+ + 1]$ at m/z : 253 and 254, respectively.



Scheme 3: Synthesis of derivatives **7** and **8a-c**.

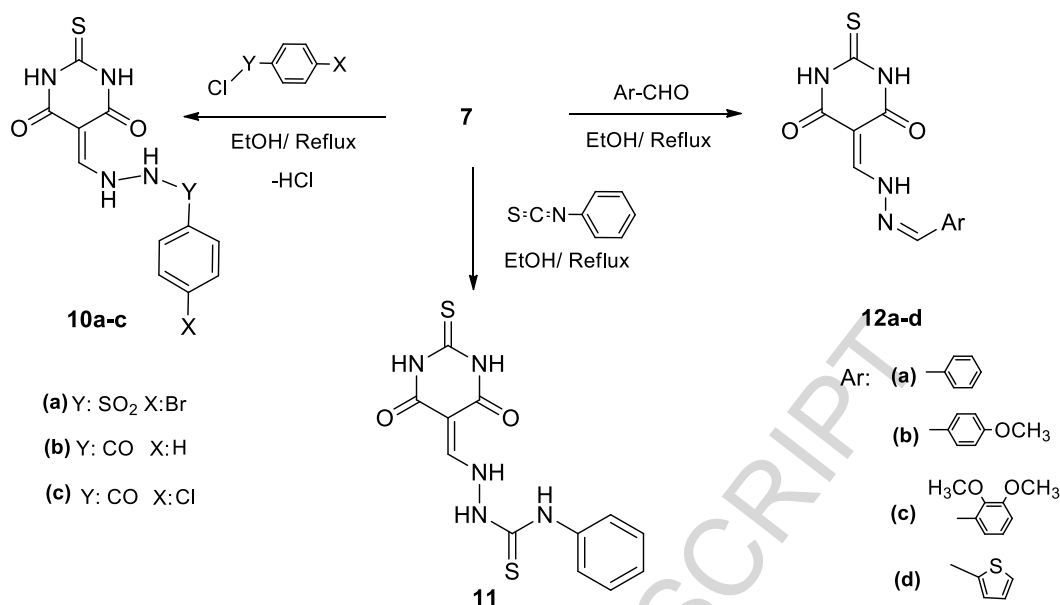
Reacting equimolar ratio of **2** and hydrazinylmethylidene pyrimidine **7** in refluxing ethanol afforded *N,N*-bis(5-methylidene-2-thioxo-dihydropyrimidine-4,6(1*H*,3*H*)-dione)hydrazine **9**. Noticeably, compound **9** was not successfully obtained upon treating the precursor **2** with hydrazine hydrate in 2:1 mole equivalence (**Scheme 4**). Elemental and spectral data supported the assigned structure of bis-pyrimidine hydrazine derivative **9**.



Scheme 4: Synthesis of derivative **9**.

Scheme 5 depicts the synthesis of derivatives **10a-c**, **11** and **12a-d**. Reaction of hydrazinylmethylidenepyrimidine **7** with bromobenzenesulfonyl chloride or benzoyl chlorides adopting the reported method^[27] furnished the corresponding benzenesulfonohydrazide and benzohydrazides **10a-c**, respectively. Spectral and elemental analyses were compatible with the structures of **10a-c**, for example, ¹H-NMR spectrum of **10c** showed two doublets at δ 7.60 and 7.92 ppm ($J= 7.2$ Hz) corresponding to the aromatic protons. Furthermore, compound **7** was reacted with phenyl isothiocyanate to afford the corresponding phenylthiosemicarbazide **11**. Spectral and elemental analyses ascertained the structure of **11**. ¹H-NMR spectrum of **11** showed three multiplets integrated for five aromatic protons at δ 7.05-7.10, 7.32-7.39 and 7.58-7.65 ppm. Mass spectrum showed the molecular ion peak [$M^+ + 1$] at m/z : 322.

Finally, condensation of **7** with different aromatic aldehydes in refluxing ethanol afforded benzylidenehydrazinylmethylidene derivatives **12a-d**.^[24,28-31] Compounds **12a-d** gave satisfactory analytical and spectral data in accordance with their depicted structures. ¹H-NMR of **12a** showed two signals at 7.46 ppm and 8.29 ppm assigned for the two vinylic protons. ¹H-NMR of **12b** showed the methoxy protons signal at 3.74 ppm while in **12c** the two methoxy protons appeared as two singlets at 3.80 and 3.82 ppm. ¹³C-NMR of **12c** showed the two vinylic carbons at 155.56 and 159.35 ppm while the carbonyl carbon appeared at 161.62 ppm.



Scheme 5: Synthesis of derivatives **10a-c**, **11** and **12a-d**.

2.2. Pharmacology

2.2.1 Antitumor activity

Anticancer activity of the target compounds **2**, **3a-h**, **4-7**, **8a-c**, **9**, **10a-c**, **11** and **12a-d** was evaluated against human colorectal cancer (Caco-2), hepatic cancer (HepG-2) and breast cancer (MCF-7) which were synthesized on the light of the promising anticancer activity of thiobarbiturates **V** and **VI**^[9]. Doxorubicin was used as a reference standard and showed IC₅₀ of 34.9, 4.68 and 1.17 μM against the tested cancer cell lines, respectively. A comparative structural profile between (**V**, **VI**) and the target compounds **2**, **3a-h**, **4**, **5**, **6**, **7**, **8a-c**, **9**, **10a-c**, **11** and **12a-d** was illustrated in **Figure 2**. Structural features of **V** and **VI** included non-modified moiety **A** (thiobarbituric acid motif) and modified moiety **B** (colored red and blue) with a linker of methyldiene group at C5 of thiobarbituric acid (**Figure 2**).

All the test compounds except precursor **2** showed potent anticancer activity against the screened cancer cell lines (Table 1). With regards to cytotoxicity against Caco-2 cell line, the anticancer effect of the target compounds **3a-h**, **7**, **10a-c**, **11** and **12a-d** surpassed that of doxorubicin. Among the test compounds, benzenesulfonylhydrazide **10a** was the most potent compound (IC₅₀ = 0.11 μM) compared to doxorubicin (IC₅₀ = 34.9 μM). On the other hand, the aminopyrazolone derivative **8c** showed the lowest IC₅₀ (1.14 = μM), in spite of being still 34 times more active than doxorubicin. Also, the benzohydrazide **10b** and the benzylidenehydrazinyl derivative **12a** showed equipotent activity against Caco-2 cell line (IC₅₀ = 0.16 μM each).

Similarly, Hepatic cell line HepG-2 showed high sensitivity towards the test compounds compared to doxorubicin. Comparatively, thiophenylmethylidene derivative **12d** was several folds more active than doxorubicin (IC₅₀ of 0.07 and 4.68 μM, respectively), while phenylthiosemicarbazide, **11** showed the lowest activity of IC₅₀ = 0.89 μM. Further, compounds **3a,b**, **10a,b** and **12a** explored almost half the activity of **12d** (IC₅₀ = 0.18, 0.16, 0.16, 0.14 and 0.18 μM, respectively) compared to doxorubicin. Thus these compounds recorded forty folds the activity of doxorubicin (IC₅₀ of 4.68 μM).

Simultaneously, all the test compounds except **2** showed potent anticancer activity against (MCF-7) compared to doxorubicin ($IC_{50} = 1.17 \mu\text{M}$). Among the test compounds, thiophenylmethylidene derivative **12d** ($IC_{50} = 0.08 \mu\text{M}$) was several folds more potent than doxorubicin, while *bis*-thiobarbituricpiperazine derivative **4** showed the lowest activity of $IC_{50} = 0.81 \mu\text{M}$ compared to doxorubicin. Also compounds **3a**, **3e**, **5** and **10c** almost demonstrated half the activity of **12d** ($IC_{50} = 0.15, 0.18, 0.17$ and $0.12 \mu\text{M}$, respectively), yet they were almost ten folds more active than doxorubicin.

Table 1: IC_{50} of the test set of compounds against human colorectal cancer (Caco-2), hepatic cancer (HepG-2), and breast cancer (MCF-7).

Compd #	IC_{50} (μM)		
	Caco-2	HepG-2	MCF-7
2	N.A. ^a	N.A.	N.A.
3a	0.57 ^b	0.18	0.15
3b	0.24	0.16	0.28
3c	0.64	0.71	0.53
3d	0.32	0.29	0.26
3e	0.26	0.28	0.18
3f	0.36	0.52	0.45
3g	0.39	0.46	0.36
3h	0.24	0.29	0.24
4	0.91	0.79	0.81
5	0.23	0.21	0.17
6	0.51	0.52	0.42
7	0.74	0.52	0.35
8a	0.18	0.25	0.57
8b	0.38	0.63	0.33
8c	1.14	0.66	0.36
9	0.51	0.37	0.27
10a	0.11	0.16	0.23
10b	0.16	0.14	0.27
10c	0.52	0.40	0.12
11	0.4	0.89	0.58
12a	0.16	0.18	0.32
12b	0.36	0.49	0.35
12c	0.70	0.56	0.41
12d	0.46	0.07	0.08
Doxorubicin	34.9	4.68	1.17

^a N.A. = Not active

^b IC_{50} values are the average of 3 independent runs.

2.3. Structural Design and Structure Activity Relationship (SAR)

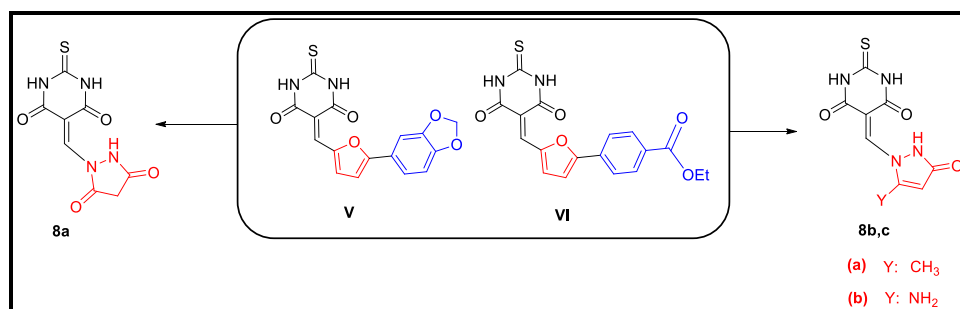
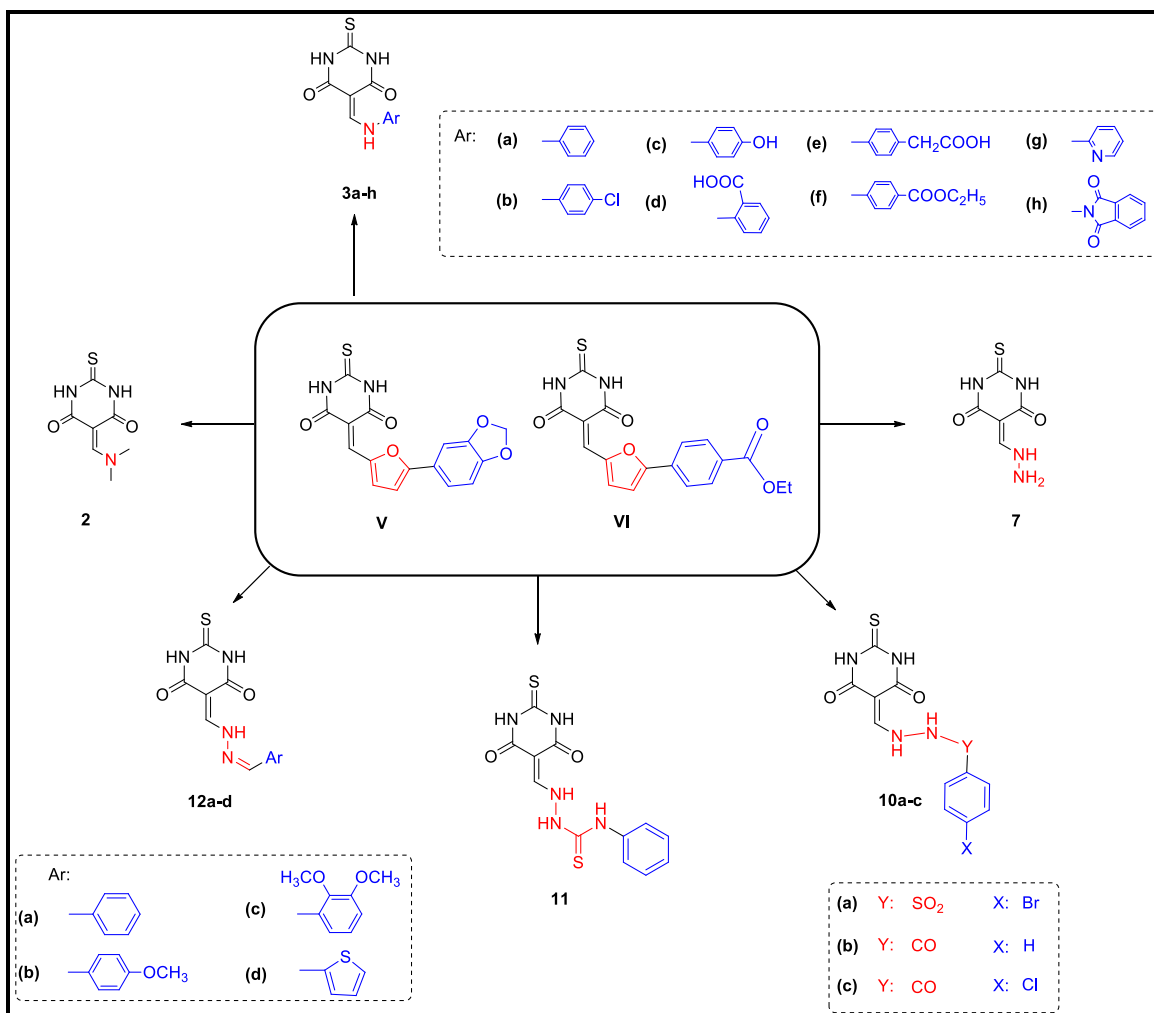
Compounds **V** and **VI** were adopted as structural leads for design of new compounds in this study (figure 2). Molecular manipulations performed aimed to examine the effect of replacement of the arylfuranly moiety by classical and non-classical bioisosteres. Also attempted was the synthesis of bis-compounds with double thiobarbiturate warheads. Replacement of the heteroaryl moiety **B** of **V** and **VI** with dimethylamino moiety in precursor **2**, completely abolished the anticancer activity

reflecting the possible need for a hydrogen bond donor and/or an aromatic side chain linked to the thiobarbiturate ring for activity. Subsequently, **2** was derivatized to furnish the compounds in this study **3a-h**, **4-7**, **8a-c**, **9**, **10a-c**, **11** and **12a-d**. All adopted synthetic modifications retrieved the cytotoxic activity of these series. Structural modification profiling of modified moiety *B* of the test compounds demonstrates variable hydrophilic/hydrophobic and hydrogen bond donor/acceptor characters.

First, derivatives **3a-h** had their aryl/heteroaryl terminal rings attached through an amino group to the thiobarbiturate warhead in place of the furan ring in **V** and **VI**. The hydrazinyl analog **7** and its arylidene derivatives **12a-c** had an aliphatic/hydrogen bond donor linker. A highlight was the thienylmethylidene derivative **12d** that was several times more potent than doxorubicin against Caco-2 ($IC_{50} = 0.46 \mu\text{M}$), HepG-2 ($IC_{50} = 0.07 \mu\text{M}$) and MCF-7 ($IC_{50} = 0.08 \mu\text{M}$) and thus the most potent compound in this study. Replacement of the terminal methylidene group by a hydrogen bond acceptor moiety in **10a-c**, C=O or SO₂, lead to enhanced potency. Linker length extension in **11** was much in favor of cytotoxicity. (Figure 2, upper panel)

Elimination of the terminal aryl ring and replacement of the furan ring by a pyrazoline or pyrazolidine ring decorated with hydrogen bond donor/acceptor groups furnished derivatives **8a-c** with retained but moderate to low efficacy. (Figure 2, middle panel)

Finally, synthesis of derivatives with double thiobarbiturate warheads and with variable aromatic/cyclic or acyclic aliphatic diamine linkers furnished compounds **4-6** and **9**. While this strategy didn't display specific enhancement in activity, the most potent derivative was that with the aromatic phenylenediamine linker (compound **5**). Compound **9**, with the hydrazinyl linker, was less potent than **5**, but the least potent in this series were derivatives **4** and **6** having alicyclic or aliphatic diamine linker groups, respectively. (Figure 2, lower panel)



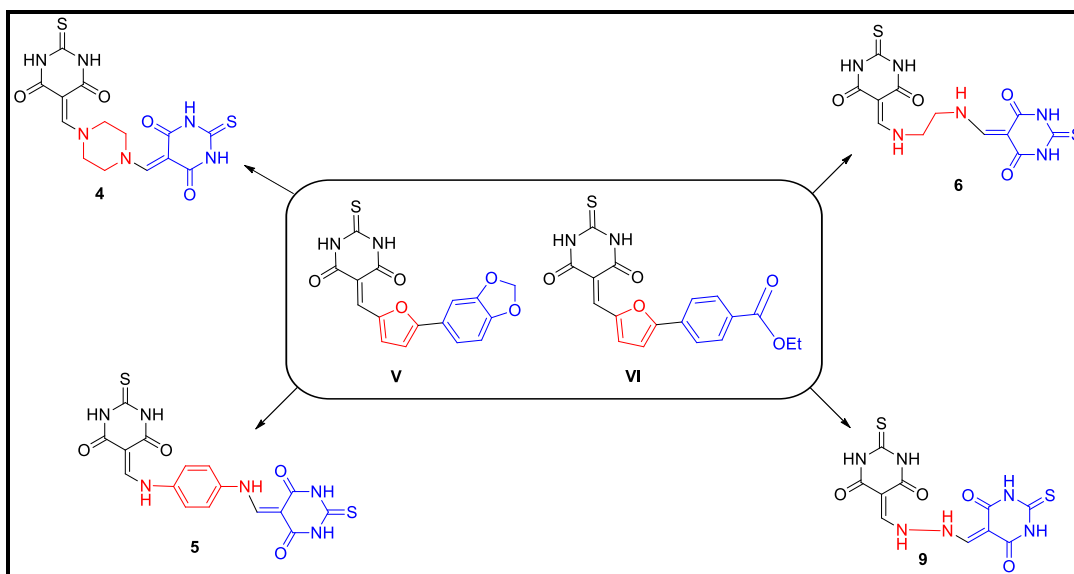


Figure 2: Structural design of the target thiobarbiturate derivatives. Fragment replacement profile of reported thiobarbiturates (**V**, **VI**) and designed thiobarbituric acid derivatives as antitumor. First modification (upper panel) in compounds **2**, **3a-h**, **7**, **10a-c**, **11** and **12a-d**, moiety **B** was replaced by different amines e.g. amino group, hydrazone, hydrazinocarbonyl, hydrazinosulfone and thiosemicarbazide moieties. Second modification in compounds **8a-c** (middle panel) explored isosteric replacement of furan ring by pyrazole moiety. Third modification (lower panel) for compounds **4-6** and **9** included replacing moiety **B** in **V** and **VI** with aliphatic/aryl diamine linker to obtain bis-thiobarbiturates.

2.4. Quantitative Structure Activity Relationship (QSAR)

A group of eighteen compounds with a variety in structure and IC_{50} values was used as a training set to build a pharmacophore model based on their 2D descriptors. The built in set of 180 2D-descriptors in MOE (version 2016.08)^[32] was calculated for all the compounds. Weka (version 3.8.3)^[33-34] and MOE analysis were used to filter the most important 2D-descriptors. Those selected as most influential were utilized for building various pharmacophore models by MOE by making alternatives of all sets and further filtration by exclusion of the least important descriptors.

The best predicting model consisted of four 2D descriptors of two different types; adjacency and distance matrix descriptors (BCUT_SMR_0) and partial charge descriptors (PEOE_VSA-2, PEOE_VSA+3 and PEOE_VSA_FNEG) (more details about the descriptors are provided in the supplementary material section). Statistically, the best model showed correlation coefficient of 75.55% ($r^2 = 0.7555$), an internal predictive power by cross validation of 64% with XRMSE= 0.1818, ($r^2 = 0.6402$) (Table 2 and figure 3). It also displayed a predictive power of the external test set (6 compounds) of 70.44% ($r^2 = 0.7044$) (Table 3 and figure 4).

The estimated linear regression equation of the model is:

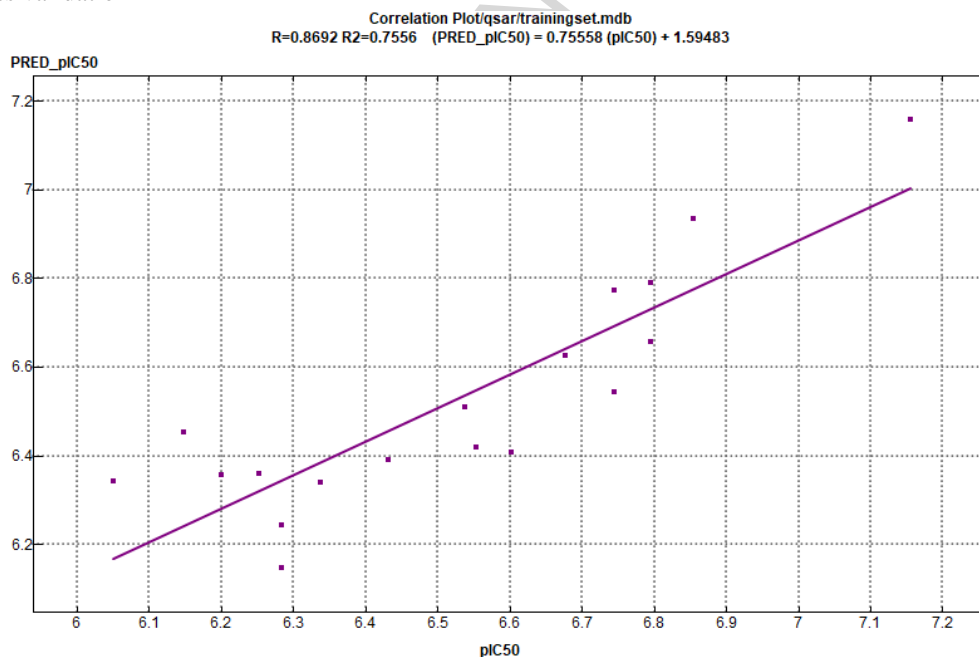
$$pIC_{50} = 8.01089 + (1.42041 * BCUT_SMR_0) + (2.68121 * PEOE_VSA_FNEG) + (0.02087 * PEOE_VSA+3) + (0.01037 * PEOE_VSA-2)$$

The equation shows that all the four descriptors correlate positively with pIC_{50} .

Table 2: Compounds in the training set with their pIC_{50} values (MCF-7 cell line), predicted pIC_{50} , residuals and Z-scores.

Compd #	pIC_{50}	PRED pIC_{50}	RES	Z-SCORE	XPRED*	XRES*	XZ-SCORE*
3a	6.74	6.54	0.20	1.42	6.52	0.23	1.68
3b	6.80	6.66	0.14	0.98	6.62	0.17	1.21
3c	6.15	6.45	-0.30	2.13	6.49	-0.34	2.72
3d	6.54	6.51	0.03	0.19	6.51	0.03	0.21
3e	6.55	6.42	0.13	0.94	6.40	0.15	1.05
3g	6.34	6.34	0.00	0.02	6.34	0.00	0.02
5	6.68	6.63	0.05	0.36	6.61	0.07	0.46
6	6.28	6.24	0.04	0.29	5.96	0.32	2.23
7	6.28	6.15	0.14	0.96	6.09	0.19	1.38
8a	6.60	6.41	0.20	1.38	6.38	0.22	1.61
8b	6.20	6.36	-0.16	1.10	6.37	-0.17	1.23
9	6.43	6.39	0.04	0.29	6.38	0.05	0.38
10a	6.80	6.79	0.01	0.04	6.78	0.01	0.08
10b	6.85	6.94	-0.08	0.57	7.01	-0.16	1.09
11	6.05	6.34	-0.29	2.06	6.38	-0.33	2.63
12a	6.74	6.77	-0.03	0.20	6.78	-0.04	0.25
12c	6.25	6.36	-0.11	0.76	6.38	-0.12	0.86
12d	7.15	7.16	0.00	0.02	7.18	-0.03	0.18

* X: cross validation

**Figure 3:** Correlation plot of the training set showing R^2 value = 0.755**Table 3:** Compounds in the test set with their pIC_{50} values (MCF-7 cell line), predicted pIC_{50} and the residual values.

Compd #	pIC_{50}	PRED pIC_{50}	RES
3f	6.28	6.29	0.01
3h	6.54	6.74	0.20
4	6.10	5.92	-0.19
8c	6.18	6.27	0.09
10c	6.40	7.03	0.63

12b	6.31	6.57	0.26
------------	------	------	------

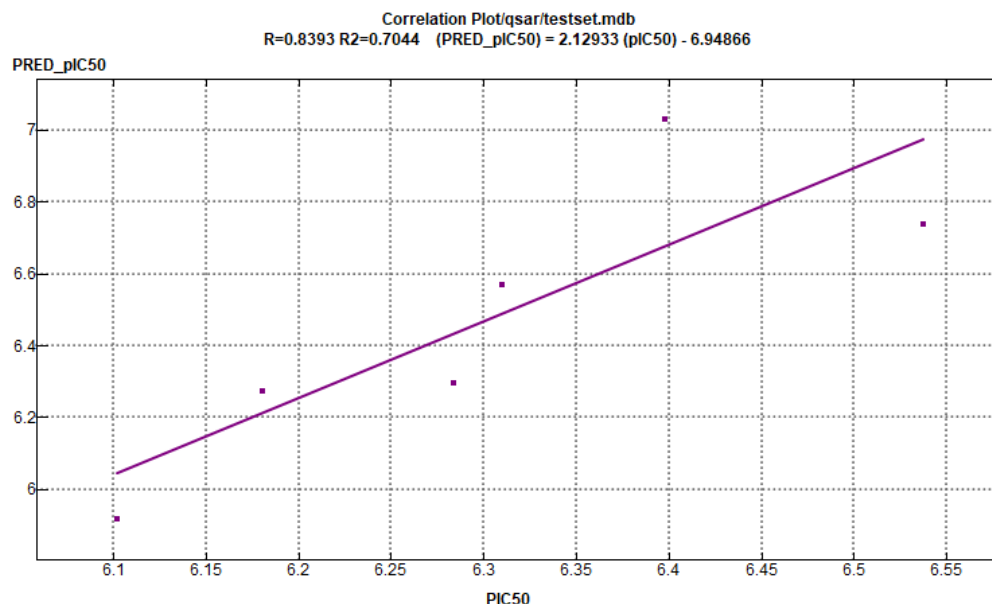


Figure 4: Correlation plot of the test set showing R^2 value= 0.704

2.5. Pharmacophore

For building the pharmacophore model, 15 compounds of thiobarbiturates were energy minimized using the MMFFX94 forcefield and a gradient of 0.01 RMSD in MOE (version 2016.08). Alignment of the energy minimized molecules was then performed followed by pharmacophore model building.

The model was built based on five main common structural features; PiR | Aro | Hyd, Acc, Acc, Hyd & Don. For the internal validation, the model was able to identify all the compounds in the test set except for the doxorubicin, which was expected because it represents a different chemotype (Figures 5&6).

For external validation, OTAVA RNA binding database^[35] was used as a decoy database to test the model accuracy. It picked up only 127 out of 2775 as actives (a low percentage of 4.5%). This step assures the model's selectivity.

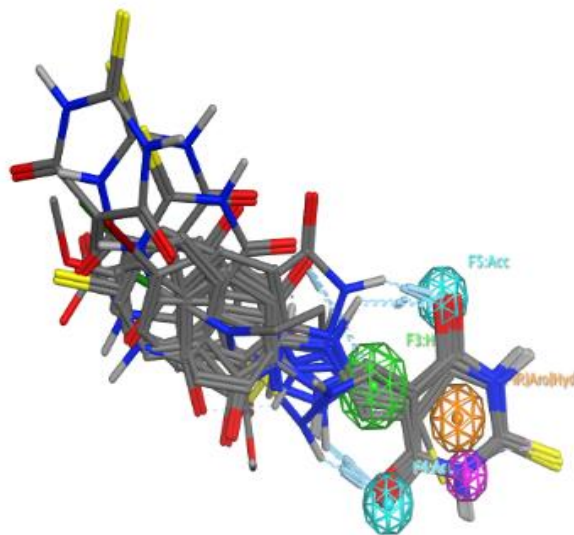


Figure 5: Five features of the pharmacophore model on the 15 aligned compounds.

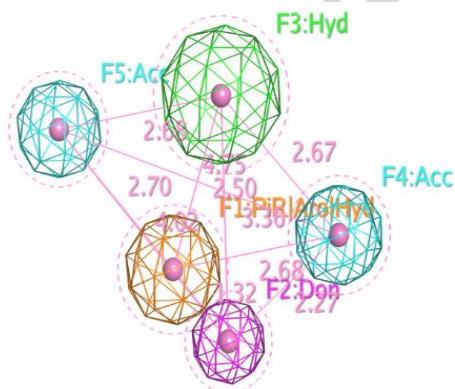


Figure 6: 3D spatial distribution of the five pharmacophoric features.

2.6. In silico physicochemical and ADME properties prediction

The results of drug likeness and ADME prediction using SwissADME^[36] are summarized in table 4 and table 5, respectively.

With regards to drug likeness (table 4), most of the compounds have zero violation for Lipinski's rule for oral drugs, except for three compounds (**5**, **6** & **9**) which have only one violation (HBD >5) yet with which they still lie in the category of orally bioavailable compounds. For Doxorubicin, it displayed 3 violations (HBD >5, HBA >10 and MWt >500). Most of TPSA values were less than 200 Å², except for the three compounds (having HBD violations) and Doxorubicin which were found to be slightly higher than 200 Å². Rotatable bonds are any single bonds not in a ring, attached to a heavy atom (non-hydrogen). All compounds have between 1 to 5 rotatable bonds which is in favor of binding to their biotarget to avoid entropic penalty.

Table 4: Drug-likeness based on Lipinski's rule of five, TPSA and number of rotatable bonds

Molecule	HBD	HBA	MlogP	# of violations*	TPSA	# of rot. bonds
----------	-----	-----	-------	------------------	------	-----------------

3a	3	2	-0.36	0	102.32	2
3b	3	2	0.6	0	102.32	2
3c	4	3	-0.9	0	122.55	2
3d	4	4	-1.79	0	139.62	3
3e	4	4	-0.68	0	139.62	4
3f	3	4	-0.15	0	128.62	5
3g	3	3	-1.05	0	115.21	2
3h	3	4	-0.46	0	139.7	2
4	4	4	-2.62	0	187.06	2
5	6	4	-1.8	1	204.64	4
6	6	4	-3.15	1	204.64	5
7	4	3	-2.35	0	128.34	1
8a	3	4	-2.23	0	139.7	1
8b	3	3	-1.25	0	128.08	1
8c	4	3	-1.68	0	154.1	1
9	6	4	-2.91	1	204.64	3
10a	4	5	-0.19	0	156.87	4
10b	4	3	-0.55	0	131.42	4
10c	4	3	0.4	0	131.42	4
11	5	2	-0.55	0	158.47	5
12a	3	3	-0.42	0	114.68	3
12b	3	4	-0.68	0	123.91	4
12c	3	5	-0.94	0	133.14	5
12d	3	3	-0.55	0	142.92	3
Doxorubicin	6	12	-2.1	3	206.07	5

*Violations considering MlogP, HBD, HBA and compound's MWt (<500)

With regards to the pharmacokinetic properties and medicinal chemistry parameters of the new compounds (table 5), it was found that there are nine compounds (**3a-c**, **3f**, **3g**, **10c** and **12a-c**) having high gastrointestinal absorption compared to low absorption of doxorubicin. Also, all compounds have no permeation to the blood brain barrier, thus ensuring that these systemically targeted molecules will have low to no CNS side effects. The rate of GIT absorption and permeability of BBB was predicted according to Boiled-Egg theory, where the yolk represents BBB permeable compounds and the white represents GI absorption.

All the compounds, according to a SVM model with accuracy of 0.72 in internal validation and 0.88 in external validation, were found to be poor substrates for P-glycoprotein (P-gp) except for the Doxorubicin. Hence, the bioavailability scores were found to be higher in all compounds than Doxorubicin.

In Pan-interference compounds assay (PAINS) structural alerts, all the compounds along with Doxorubicin were found to have only one structural alert (quinone A for doxorubicin and ene_six_het_A for other compounds). Though PAINS are important features to be considered while developing drugs to avoid false positives results, yet over estimation and blind use of these filters might only lead to exclusion of promising hits based on phantom PAINS^[37]

Synthetic accessibility score shows that thiobarbiturates in this study are more synthetically feasible (score = 2.19-3.14) than doxorubicin (score = 5.81). The scores range from

1 (very easy) to 10 (very difficult) based on a model with $r^2=0.94$, which depends on analyzing the information of already synthesized molecules and their structure complexity.

Table 5: Pharmacokinetics and medicinal chemistry parameters.

Molecule	GI absorption	BBB permeation	Pgp substrate	Bioavailability score	PAINS alerts	Synthetic Accessibility
3a	High	No	No	0.55	1	2.34
3b	High	No	No	0.55	1	2.34
3c	High	No	No	0.55	1	2.3
3d	Low	No	No	0.56	1	2.36
3e	Low	No	No	0.56	1	2.4
3f	High	No	No	0.55	1	2.53
3g	High	No	No	0.55	1	2.57
3h	Low	No	No	0.55	1	2.5
4	Low	No	No	0.55	1	3.14
5	Low	No	No	0.55	1	2.8
6	Low	No	No	0.55	1	3.04
7	Low	No	No	0.55	1	2.19
8a	Low	No	No	0.55	1	2.99
8b	Low	No	No	0.55	1	2.6
8c	Low	No	No	0.55	1	2.68
9	Low	No	No	0.55	1	2.81
10a	Low	No	No	0.55	1	2.76
10b	Low	No	No	0.55	1	2.49
10c	High	No	No	0.55	1	2.5
11	Low	No	No	0.55	1	2.81
12a	High	No	No	0.55	1	2.63
12b	High	No	No	0.55	1	2.63
12c	High	No	No	0.55	1	2.9
12d	Low	No	No	0.55	1	2.81
Doxorubicin	Low	No	Yes	0.17	1	5.81

3. Conclusion

In conclusion, thiobarbiturate derivatives **3a-h**, **4**, **5**, **6**, **7**, **8a-c**, **9**, **10a-c**, **11** and **12a-d** were synthesized. Structural profile of the target compounds incorporated methyldiene moiety at C5 that in turn carried different aryl/heteroaryl groups. They were tested for anticancer activity against three cancer cell lines e.g. Caco-2, HepG-2 and MCF-7. All the test compounds were greatly more active than doxorubicin. Comparatively, Compound **12d** was remarkably the most potent one against HepG-2 and MCF-7. Furthermore, both a QSAR and pharmacophore model was built for these derivatives and were highly reliable in terms of predictivity and selectivity, respectively.

4. Materials and Methods

4.1. Chemistry

All chemicals and reagents used in the current study were of analytical grade. TLC using percolated Aluminium sheets silica gel Merck 60 F 254 and were visualized by UV lamp. Melting points were measured in open capillary tubes using Griffin apparatus. The infrared (IR) spectra were

recorded using potassium bromide disc technique on Shimadzu 435 IR Spectrophotometer Bruker ATR/ FTIR Spectrophotometer. All the proton nuclear magnetic resonance ($^1\text{H-NMR}$) spectra and the carbon nuclear magnetic resonance ($^{13}\text{C-NMR}$) spectra were performed on Varian Gemini 300 MHz Spectrophotometer using tetramethylsilane (TMS) as internal standard. Chemical shift values (δ) are given using parts per million scale (ppm). Mass spectra were recorded on DI-50 unit of Shimadzu GC/MS-QP 5050A, Hewlett Packard 5988 Spectrometer and Direct Insertion Probe MS 5975 mass selective detector. Elemental analyses (C,H,N) were performed by Micro Analytical Center, *In-vitro* anticancer screening was performed by The Regional Center for Mycology and Biotechnology, Al-Azhar University.

4.1.1. 5-[(Dimethylamino)methylidene]-2-thioxodihydropyrimidine-4,6(1H,3H)-dione (2)

A mixture of equimolar amounts of thiobarbituric acid (0.01 mol) and dimethylamidedimethylacetal (0.01 mol) in dry benzene with few drops of piperidine was stirred for 5 h at room temperature. The precipitate was filtered and crystallized from dry benzene.

Yield (95 %), **mp.** 180-182 °C. IR (KBr) (cm^{-1}): 3102 (NH); 1603 (CO). $^1\text{H-NMR}$ (DMSO- d_6 , D_2O) δ 3.50 (s, 6H, 2CH₃); 7.88 (s, 1H, CH); 11.28 (s, 2H, 2NH exchangeable with D_2O). MS m/z (%): 199 (M^+ , 5.46); 144 (100.00). Anal. Calcd for $\text{C}_7\text{H}_9\text{N}_3\text{O}_2\text{S}$ (199.23): C, 42.20; H, 4.55; N, 21.09%. Found: C, 42.06; H, 4.51; N, 20.87%.

4.1.2. General procedure for the synthesis of Dihydro-5-[(arylamino)methylidene]-2-thioxopyrimidine-4,6(1H,3H)-dione (3 a-h)

A mixture of equimolar amounts of **2** and the appropriate aromatic amine (0.01 mol) in ethanol was refluxed for 2-5 h. The mixture was allowed to cool; the solid product was filtered and crystallized from ethanol.

4.1.2.1. 5-[(Phenylamino)methylidene]-2-thioxo-dihydropyrimidine-4,6(1H,3H)-dione (3a)

Yield (40%), **mp.** 254-257 °C. IR (KBr) (cm^{-1}): 3100 (NH); 1685 (CO). $^1\text{H-NMR}$ (DMSO- d_6 , D_2O) δ 6.47-6.51 (m, 1H, 4-CH Ar); 6.52-6.55 (m, 2H, 3,5-CH Ar); 6.96-7.01 (m, 2H, 2,6-CH Ar); 8.19 (s, 1H, =CH); 10.27 (s, 3H, 3NH exchangeable with D_2O). MS m/z (%): 249 ($\text{M}^+ + 2$, 11.01); 51 (100). Anal. Calcd for $\text{C}_{11}\text{H}_9\text{N}_3\text{O}_2\text{S}$ (247.27): C, 53.43; H, 3.67; N, 16.99%. Found: C, 53.64; H, 3.71; N, 17.18%.

4.1.2.2. 5-[(4-Chlorophenylamino)methylidene]-2-thioxo-dihydropyrimidine-4,6(1H,3H)-dione (3b)

Yield (38%), **mp.** 251-254 °C. IR (KBr) (cm^{-1}): 3108 (NH); 1687 (CO). $^1\text{H-NMR}$ (DMSO- d_6 , D_2O) δ 6.53, 6.99 (2d, 4H Ar, $J=6.6$ Hz); 8.2 (s, 1H, =CH); 10.29 (s, 2H, 2NH exchangeable with D_2O); 11.4 (s, 1H, NH exchangeable with D_2O). $^{13}\text{C-NMR}$ (DMSO- d_6) δ 102.95 (C5 thiobarbituric); 115.13 (2C, C2, 6Ar); 128.41(2C, C3,5 Ar); 147.64 (C4Ar); 148.51 (C1 Ar); 163.75 (=CH-NH); 174.19 (2C, 2C=O); 176.42 (C=S). MS m/z (%): 281 (M^+ , 100). Anal. Calcd for $\text{C}_{11}\text{H}_8\text{ClN}_3\text{O}_2\text{S}$ (281.72): C, 46.90; H, 2.86; N, 14.92%. Found: C, 47.08; H, 2.84; N, 15.13%.

4.1.2.3. 5-[(4-Hydroxyphenylamino)methylidene]-2-thioxo-dihydropyrimidine-4,6(1H,3H)-dione (3c)

Yield (68 %), **mp.** 226-229 °C. IR (KBr) (cm⁻¹): 3404 (OH); 3191 (NH); 1655 (CO). ¹H-NMR (DMSO-d₆, D₂O) δ 6.79, 7.34 (2d, 4H Ar, *J*=9 Hz); 8.42 (s, 1H, =CH-N); 9.80 (s, 1H, OH exchangeable with D₂O); 10.15 (s, 1H, NH exchangeable with D₂O); 11.20 (s, 2H, 2NH exchangeable with D₂O). MS *m/z* (%): 263 (M⁺, 100.00). Anal. Calcd for C₁₁H₉N₃O₃S (263.27): C, 50.18; H, 3.45; N, 15.96%. Found: C, 50.32; H, 3.49; N, 16.14%.

4.1.2.4. 2-[(4,6-Dioxo-2-thioxo-tetrahydropyrimidin-5(6H)ylidene)methylamino]benzoic acid (3d)

Yield (96 %), **mp.** 277-281 °C. IR (KBr) (cm⁻¹): 3465 (OH); 3200 (NH); 1690 (COO); 1653 (CO). ¹H-NMR (DMSO-d₆, D₂O) δ 6.49-6.54 (m, 1H, 5-CH Ar); 6.68 (d, 1H, 3-CH Ar); 7.18-7.23 (m, 1H, 4-CH Ar); 7.59-7.67 (m, 1H, 6-CH Ar); 8.18 (s, 1H, =CH-N); 10.10 (s, 1H, NH exchangeable with D₂O); 10.99 (s, 2H, 2NH, exchangeable with D₂O); 15.98 (s, 1H, OH exchangeable with D₂O). MS *m/z* (%): 291 (M⁺, 6.55); 64 (100.00). Anal. Calcd for C₁₂H₉N₃O₄S (291.28): C, 49.48; H, 3.11; N, 14.43 %. Found: C, 49.62; H, 3.15; N, 14.61%.

4.1.2.5. 2-{4-[(4,6-Dioxo-2-thioxo-tetrahydropyrimidin-5(6H)-ylidene)methylamino]phenyl}-acetic acid (3e)

Yield (43 %), **mp.** 296-299 °C. IR (KBr) (cm⁻¹): 3281 (OH); 3192 (NH); 1731(COO); 1685 (CO). ¹H-NMR (DMSO-d₆, D₂O) δ 3.59 (s, 2H, CH₂); 6.56, 6.92 (2d, 4H Ar, *J*=8.1 Hz); 8.55 (d, 1H, =CH-N); 12.00 (s, 2H, 2NH exchangeable with D₂O); 12.04 (s, 1H, NH exchangeable with D₂O); 12.13 (s, 1H, OH exchangeable with D₂O). MS *m/z* (%): 305 (M⁺, 25.85); 59(100.00). Anal. Calcd for C₁₃H₁₁N₃O₄S (305.31): C, 51.14; H, 3.63; N, 13.76%. Found: C, 51.28; H, 3.68; N, 13.83%.

4.1.2.6. Ethyl-4-[(4,6-dioxo-2-thioxo-tetrahydropyrimidin-5(6H)-ylidene)methylamino]benzoate (3f)

Yield (47 %), **mp.** >300 °C. IR (KBr) (cm⁻¹): 3199 (NH); 1708 (COO); 1680 (CO). ¹H-NMR (DMSO-d₆, D₂O) δ 1.30 (t, 3H, CH₂CH₃, *J*=7.2 Hz); 4.27 (q, 2H, CH₂CH₃, *J*=7.2 Hz); 7.67, 7.97 (2d, 4H Ar, *J*=8.4Hz); 8.62 (s, 1H, =CH-N); 11.37 (s, 1H, NH exchangeable with D₂O); 12.08 (s, 2H, 2NH exchangeable with D₂O). ¹³C-NMR (DMSO-d₆) δ 14.31 (CH₂CH₃); 60.74 (CH₂CH₃); 95.04 (C5 thiobarbituric); 118.58 (2C, C2,6 Ar); 127.04 (C4 Ar); 130.71 (2C, C3,5 Ar); 142.05 (CH-NH); 151.79 (C1 Ar); 161.40 (C=O ester); 163.72 (C=O thiobarbituric); 165.81 (C=O thiobarbituric); 177.92 (C=S). MS *m/z* (%): 319 (M⁺, 100.00). Anal. Calcd for C₁₄H₁₃N₃O₄S (319.34): C, 52.66; H, 4.10; N, 13.16 %. Found: C, 52.89; H 4.17; N, 13.38%.

4.1.2.7. 5-[(Pyridin-2-ylamino)methylen]-2-thioxo-dihydropyrimidine-4,6(1H,3H)-dione (3g)

Yield (54 %), mp. 222-226 °C. IR (KBr) (cm⁻¹): 3252 (NH); 1654 (CO). ¹H-NMR (DMSO-d₆, D₂O) δ 6.41-6.48 (m, 1H, 5-CH Ar); 7.32-7.38 (m, 1H, 4-CH Ar); 7.60 (d, 1H, 3-CH Ar); 7.88 (s, 1H, 6-CH Ar); 8.20(s, 1H, =CH-N); 10.23 (s, 1H, NH exchangeable with D₂O); 11.37 (s, 2H, 2 NH exchangeable with D₂O). MS *m/z* (%): 248 (M⁺, 48.50); 79 (100.00). Anal. Calcd for C₁₀H₈N₄O₂S (248.26): C, 48.38; H, 3.25; N, 22.57%. Found: C, 48.5; H, 3.28; N, 22.69%.

4.1.2.8. 2-[(4,6-Dioxo-2-thioxo-tetrahydropyrimidin-5(6H)-ylidene)methylamino] isoindoline-1,3-dione (3h)

Yield (98 %), mp. 340-341 °C. IR (KBr) (cm⁻¹): 3227 (NH); 1656 (CO). ¹H-NMR (DMSO-d₆, D₂O) δ 7.86-7.93 (m, 4H Ar); 8.28 (s, 1H, =CH-N); 11.66 (s, 1H, NH exchangeable with D₂O); 11.93 (s, 2H, 2NH exchangeable with D₂O). MS *m/z* (%): 315 (M⁺-1); 75 (100.00). Anal. Calcd for C₁₃H₈N₄O₄S (316.29): C, 49.37; H, 2.55; N, 17.71%. Found: C, 49.62; H, 2.59; N, 17.84%.

4.1.3. General procedure for the synthesis of Bis[2-thioxo-dihydropyrimidine-4,6(1H,3H)-dione] derivatives (4-6)

A mixture of compound **2** (0.02 mol) and appropriate aromatic diamine (0.01 mol) in ethanol was refluxed for 3-5h. The mixture was allowed to cool and the solid product was filtered and crystallized from ethanol.

4.1.3.1. N,N-Bis[5-methylidene-2-thioxo-dihydropyrimidine-4,6(1H,3H)-dione]piperazine (4)

Yield (44%), mp. 295-298 °C. IR (KBr) (cm⁻¹): 3180 (NH); 1613 (CO). ¹H-NMR (DMSO-d₆, D₂O) δ 3.07-3.09 (m, 8H, piperazine); 8.19 (s, 2H, 2 =CH-N); 11.4 (s, 4H, 4NH exchangeable with D₂O). MS *m/z* (%): 395 (M⁺+1, 0.24); 144 (100.00). Anal. Calcd for C₁₄H₁₄N₆O₄S₂ (394.43): C, 42.63; H, 3.58; N, 21.31 %. Found: C, 42.74; H, 3.61; N, 21.40%.

4.1.3.2. N,N-Bis[5-methylidene-2-thioxo-dihydropyrimidine-4,6(1H,3H)dione]phenylene-1,4-diamine (5)

Yield (50 %), mp. 139-141 °C. IR (KBr) (cm⁻¹): 3226 (NH); 1620 (CO). ¹H-NMR (DMSO-d₆, D₂O) δ 4.32 (s, 4H, 4NH exchangeable with D₂O); 5.34 (s, 2H, 2NH exchangeable with D₂O); 6.61, 7.16 (2d, 4H Ar, *J* = 8.7 Hz); 8.38 (s, 2H, 2 =CH-N). MS *m/z* (%): 416 (M⁺, 0.1); 69 (100). Anal. Calcd for C₁₆H₁₂N₆O₄S₂ (416.43): C, 46.15; H, 2.90; N, 20.18% Found: C, 46.31; H, 2.93; N, 20.39%.

4.1.3.3. N,N-Bis[5-methylidene-2-thioxo-dihydropyrimidine-4,6(1H,3H)-dione]ethylene-1,2-diamine (6)

Yield (76%), mp.>250 °C. IR (KBr) (cm⁻¹): 3183 (NH); 1620 (CO). ¹H-NMR (DMSO-d₆, D₂O) δ 2.99-3.03 (m, 4H, 2CH₂); 4.07(s, 2H, 2NH exchangeable with D₂O); 8.08 (s, 2H, 2 =CH-N); 8.92 (s, 4H, 4NH exchangeable with D₂O). MS *m/z* (%): 368 (M⁺, 43.1); 57

(100.00). Anal. Calcd for $C_{12}H_{12}N_6O_4S_2$ (368.39): C, 39.12; H, 3.28; N, 22.81%. Found: C, 38.98; H, 3.22; N, 22.67%.

4.1.4. 5-(Hydrazinylmethylidene)-2-thioxo-dihydropyrimidine-4,6(1H,3H)-dione (7)

A mixture of of **2** (0.01 mol) and hydrazine hydrate (0.01 mol) in ethanol (10 ml) was refluxed for 1h. The solution was allowed to cool and the precipitated solid product was filtered and crystallized by ethanol.

Yield (93 %), mp. $>320^\circ\text{C}$. IR (KBr) (cm^{-1}): 3279, 3110 (NH, NH_2); 1621 (CO). $^1\text{H-NMR}$ (DMSO- d_6 , D_2O) δ 7.90 (s, 3H, NH- NH_2 , exchangeable with D_2O); 8.03 (s, 1H, =CH-N); 9.45 (s, 2H, 2 NH exchangeable with D_2O). MS m/z (%): 186 (M^+ , 10.12); 144 (100.00). Anal. Calcd for $C_5H_6N_4O_2S$ (186.19): C, 32.25; H, 3.25; N, 30.09%. Found: C, 32.39; H, 3.28; N, 30.29%.

4.1.5. General procedure for the synthesis of 5-[(3,5-Dioxopyrazolidin-1-yl)methylidene]-2-thioxo-dihydropyrimidine-4,6(1H,3H)-dione (8a) and 5-[(5-Substituted-3-oxo-2,3-dihydropyrazol-1-yl)methylidene]-2-thioxo-dihydropyrimidine-4,6(1H,3H)-dione (8b,c):

Equimolar amounts of **7** (0.01 mol) and the appropriate active methylidene derivative (0.01 mol) were mixed in glacial acetic acid (or dry DMF) and refluxed for 5-10 h. The mixture was allowed to cool and the precipitated solid product was filtered and crystallized from ethanol.

4.1.5.1. 5-[(3,5-Dioxopyrazolidin-1-yl)methylidene]-2-thioxo-dihydropyrimidine-4,6(1H,3H)-dione (8a)

Yield (43%), mp. $>290^\circ\text{C}$. IR (KBr) (cm^{-1}): 3105 (NH); 1660 (CO). $^1\text{H-NMR}$ (DMSO- d_6 , D_2O) δ 2.89 (s, 2H, CH_2); 4.26 (s, 3H, 3NH exchangeable with D_2O); 7.95 (s, 1H, =CH). MS m/z (%): 254 (M^+ , 21.31); 52 (100). Anal. Calcd for $C_8H_6N_4O_4S$ (254.22): C, 37.80; H, 2.38; N, 22.04%. Found: C, 37.95; H, 2.42; N, 22.23%.

4.1.5.2. 5-[(5-Methyl-3-oxo-2,3-dihydropyrazol-1-yl)methylidene]-2-thioxo-dihydropyrimidine-4,6(1H,3H)-dione (8b)

Yield (55%), mp. 283-285 $^\circ\text{C}$. IR (KBr) (cm^{-1}): 3270 (NH); 1636 (CO). $^1\text{H-NMR}$ (DMSO- d_6 , D_2O) δ 2.22 (s, 3H, CH_3); 5.63 (s, 1H, pyrazolyl CH); 6.95 (s, 1H, =CH-N); 11.32 (s, 2H, 2NH, exchangeable with D_2O); 13.99 (s, 1H, NH, exchangeable with D_2O). $^{13}\text{C-NMR}$ (DMSO- d_6) δ 11.23 (CH_3); 89.95 (C4 pyrazolyl); 94.27 (C5 thiobarbituric); 145.18 (=CH-NH); 151.45 (C5 pyrazolyl); 158.00 (C=O pyrazolyl); 161.90 (C=O thiobarbituric); 163.00 (C=O thiobarbituric); 173.96 (C=S). MS m/z (%): 253 (M^+ , 2.31); 198 (100). Anal. Calcd for $C_9H_8N_4O_3S$ (252.25): C, 42.85; H, 3.20; N, 22.21%. Found: C, 42.91; H, 3.23; N, 22.31%.

4.1.5.3. 5-[(5-Amino-3-oxo-2,3-dihydropyrazol-1-yl)methylidene]-2-thioxo-dihydropyrimidine-4,6(1H,3H)-dione (8c)

Yield (38%), mp. $>320^\circ\text{C}$. IR (KBr) (cm^{-1}): 3278 (NH); 3184 (NH_2); 1650 (CO). $^1\text{H-NMR}$ (DMSO- d_6 , D_2O) 7.47 (s, 1H, CH pyrazolyl); 8.25 (s, 1H, =CH-N); 11.31 (s, 2H,

NH₂, exchangeable with D₂O); 11.59 (s, 1H, NH, exchangeable with D₂O); 11.88 (s, 2H, 2NH, exchangeable with D₂O). MS *m/z* (%): 254 (M⁺+1, 13.69); 99 (100). Anal. Calcd for C₈H₇N₅O₃S (253.24): C, 37.94; H, 2.79; N, 27.66%. Found: C, 37.87; H, 2.78; N, 27.52%.

4.1.6. *N,N*-Bis(5-methylidene-2-thioxo-dihydropyrimidine-4,6(1H,3H)-dione)hydrazine (9)

A mixture of equimolar amounts of **2** and the hydrazide derivative **7** (0.01 mol) was refluxed in ethanol for 5h. The mixture was allowed to cool and the solid product was filtered and crystallized by ethanol. **Yield** (69%), mp. >300 °C. IR (KBr) (cm⁻¹): 3273 (NH); 1612 (CO). ¹H-NMR (DMSO-d₆, D₂O) δ 5.83(s, 2H, 2NH exchangeable with D₂O); 8.03 (s, 2H, 2 =CH-N); 8.39 (s, 4H, 4NH exchangeable with D₂O). MS *m/z* (%): 337 (M⁺-3, 1.19); 108 (100). Anal. Calcd for C₁₀H₈N₆O₄S₂ (340.34): C, 35.29; H, 2.37; N, 24.69% Found: C, 35.38; H, 2.36; N, 24.82%.

4.1.7. General procedure for the synthesis of 4-Bromo-N'-[(4,6-dioxo-2-thioxo-tetrahydropyrimidin-5(6H)-ylidene)methyl]benzenesulfonylhydrazide (10a) N'-[(4,6-Dioxo-2-thioxo-tetrahydropyrimidin-5(6H)-ylidene)methyl]benzohydrazide derivatives (10b, 10c)

A mixture of equimolar amounts of **7** (0.01 mol) and p-bromobenzenesulfonylchloride (0.01 mol) or benzoyl chloride (0.01 mol) or p-chlorobenzoyl chloride (0.01 mol) was refluxed in ethanol for 5 h to yield compounds 10a, 10b and 10c, respectively. The mixture was allowed to cool and the solid product was filtered and crystallized first from ethanol followed by hot water.

4.1.7.1. 4-Bromo-N'-[(4,6-dioxo-2-thioxo-tetrahydropyrimidin-5(6H)-ylidene)methyl]benzenesulfonylhydrazide (10a)

Yield (39%), **mp.** 223-225 °C. IR (KBr) (cm⁻¹): 3189 (NH); 1689 (CO); 1343, 1163 (SO₂). ¹H-NMR (DMSO-d₆, D₂O) δ 7.68 -7.76 (m, 5H, 4 Ar H+ 1 =CH); 10.03-10.16 (m, 4H, 4NH, exchangeable with D₂O). MS *m/z* (%): 407 (M⁺+2, 1.47); 69 (100.00). Anal. Calcd for C₁₁H₉BrN₄O₄S₂ (405.25): C, 32.60; H, 2.24; N, 13.83%. Found: C, 32.71; H, 2.25; N, 14.01%.

4.1.7.2. N'-[(4,6-Dioxo-2-thioxo-tetrahydropyrimidin-5(6H)-ylidene)methyl]benzohydrazide (10b)

Yield (42%), **mp.** >340 °C. IR (KBr) (cm⁻¹): 3270 (NH); 1630 (CO). ¹H-NMR (DMSO-d₆, D₂O) δ 7.50-7.58 (m, 2H, 3,5-CH Ar); 7.61-7.63 (m, 1H, 4-CH Ar); 7.89-7.94 (m, 2H, 2,6-CH Ar); 8.28 (s, 1H, =CH-N); 10.62 (s, 1H, NH-CH exchangeable with D₂O); 11.38 (s, 1H, NH-CO exchangeable with D₂O); 11.95 (s, 2H, 2NH exchangeable with D₂O). MS *m/z* (%): 290 (M⁺, 2.51); 105 (100). Anal. Calcd for C₁₂H₁₀N₄O₃S (290.3): C, 49.65; H, 3.47; N, 19.30%. Found: C, 49.79; H, 3.50; N, 19.49%.

4.1.7.3. 4-Chloro-N'-[(4,6-dioxo-2-thioxo-tetrahydropyrimidin-5(6H)-ylidene)methyl]benzohydrazide (10c)

Yield (33%), **mp.** >300 °C. IR (KBr) (cm⁻¹): 3172 (NH); 1641(CO). ¹H-NMR (DMSO-d₆, D₂O) δ 5.58 (s, 2H, 2NH, exchangeable with D₂O); 7.53 (s, 1H, =CH-N); 7.60, 7.92 (2d, 4H Ar, J=7.2Hz); 10.66 (s, 2H, 2NH exchangeable with D₂O). MS *m/z* (%): 323 (M⁺-1, 4.16); 299 (100). Anal. Calcd for C₁₂H₉ClN₄O₃S (324.74): C, 44.38; H, 2.79; N, 17.25%. Found: C, 44.60; H, 2.83; N, 17.48%.

4.1.8. 1-[(Tetrahydro-4,6-dioxo-2-thioxopyrimidin-5(6H)-ylidene)methyl]-4-phenylthiosemicarbazide (11)

A mixture of equimolar amounts of **7** (0.01 mol) and phenyl isothiocyanate (0.01 mol) in ethanol was refluxed for 5 h. The mixture was allowed to cool and the solid product was filtered and crystallized from ethanol. **Yield** (64%), **mp.** 152-155 °C. IR (KBr) (cm⁻¹): 3302, 3201 (NH); 1669 (CO). ¹H-NMR (DMSO-d₆, D₂O) δ: 4.26 (s, 2H, NH-NH exchangeable with D₂O); 4.42 (s, 1H, NH-CS exchangeable with D₂O); 7.05-7.10 (m, 1H, 4-CH Ar); 7.32-7.39 (m, 2H, 3,5-CH Ar); 7.58-7.65 (m, 2H, 2,6-CH Ar); 8.39 (s, 1H, =CH); 9.03 (s, 2H, 2NH exchangeable with D₂O). MS *m/z* (%): 322 (M⁺+1, 0.25); 50 (100). Anal. Calcd for C₁₂H₁₁N₅O₂S₂ (321.38): C, 44.85; H, 3.45; N, 21.79%. Found: C, 44.97; H, 3.48; N, 21.97%.

4.1.9. General procedure for the synthesis of 5-[(2-Benzylidenehydrazinyl)methylidene]-2-thioxo-dihydropyrimidine-4,6(1H,3H)-dione derivatives (12a-c) 5-[(2-(Thiophen-2-ylmethylidene)hydrazinyl)methylidene]-2-thioxo-dihydropyrimidine-4,6(1H,3H)-dione (12d)

A mixture of equimolar amounts of **7** (0.01 mol) and the appropriate aromatic aldehyde (0.01 mol) in ethanol was refluxed for 1-3 h. The mixture was allowed to cool and the solid product was filtered and crystallized from ethanol.

4.1.9.1. 5-[(2-Benzylidenehydrazinyl)methylidene]-2-thioxo-dihydropyrimidine-4,6(1H,3H)-dione (12a)

Yield (55%), **mp.** >280 °C. IR (KBr) (cm⁻¹): 3122 (NH); 1655 (CO). ¹H-NMR (DMSO-d₆, D₂O) δ 7.46 (s, 1H, =CH-N); 7.48-7.56 (m, 3H, 3,4,5-CH Ar); 8.11 (d, 2H, 2,6-CH Ar); 8.29 (s, 1H, N=CH); 12.31 (s, 1H, NH exchangeable with D₂O); 12.43 (s, 2H, 2NH exchangeable with D₂O). ¹³C-NMR (DMSO-d₆) δ 119.12 (C5 thiobarbituric); 128.08 (2C, C3, 5Ar); 132.63 (C1 Ar); 133.37 (3C, C2,4,6 Ar); 155.56 (C=N); 159.35 (=C-N); 161.62 (2C, 2C=O); 178.56 (C=S). MS *m/z* (%): 274 (M⁺, 2.57); 135 (100). Anal. Calcd for C₁₂H₁₀N₄O₂S (274.3): C, 52.54; H, 3.67; N, 20.43%. Found: C, 52.82; H, 3.73; N, 20.67%.

4.1.9.2. 5-[(2-(4-Methoxybenzylidene)hydrazinyl)methylidene]-2-thioxo-dihydro pyrimidine-4,6(1H,3H)-dione (12b)

Yield (58%), **mp.** >250 °C. IR (KBr) (cm⁻¹): 3254 (NH); 1640 (CO). ¹H-NMR (DMSO-d₆, D₂O) δ 3.74 (s, 3H, CH₃); 6.70, 6.88 (2d, 4H Ar, J=8.7 Hz); 7.42 (d, 1H, =CH-N); 7.65 (s, 1H, N=CH); 11.5 (s, 3H, 3NH exchangeable with D₂O). MS *m/z* (%): 304 (M⁺, 12.19);

164 (100). Anal. Calcd for: C₁₃H₁₂N₄O₃S (304.32): C, 51.31; H, 3.97; N, 18.41%. Found: C, 51.48; H, 4.02; N, 18.53%.

4.1.9.3. 5-[(2-(2,3-dimethoxybenzylidene)hydrazinyl)methylidene]-2-thioxo-dihydropyrimidine-4,6(1H,3H)-dione (12c)

Yield (90%), **mp.** 278-279 °C. IR (KBr) (cm⁻¹): 3238 (NH); 1625 (CO). ¹H-NMR (DMSO-d₆, D₂O) δ 3.80,3.82 (2s, 6H, 2 OCH₃); 7.07-7.18 (m, 1H, 4-CH Ar); 7.42-7.45 (m, 1H, 5-CH Ar); 7.95-7.98 (m, 1H, 6-CH Ar); 8.47 (s, 1H, =CH-N); 8.93 (s, 1H, N=CH); 10.35 (s, H, NH exchangeable with D₂O); 12.55 (s, 2H, 2NH exchangeable with D₂O). MS *m/z* (%): 334 (M⁺, 3.28); 149 (100.00). Anal. Calcd for C₁₄H₁₄N₄O₄S (334.35): C, 50.29; H, 4.22; N, 16.76%. Found: C, 50.38; H, 4.25; N, 16.89%.

4.1.9.4. 5-[(2-(thiophen-2-ylmethylidene)hydrazinyl)methylidene]-2-thioxo-dihydropyrimidine-4,6(1H,3H)-dione (12d)

Yield (60 %), **mp.** >320 °C. IR (KBr) (cm⁻¹): 3181 (NH); 1669 (CO). ¹H-NMR (DMSO-d₆, D₂O) δ 4.32(s, 1H, NH exchangeable with D₂O); 7.12 (t, 1H, 4-CH thiophene); 7.46 (d, 1H, 3-CH thiophene); 7.62 (d, 1H, 5-CH thiophene); 7.99 (s, 1H, =CH-N); 8.41 (s, 1H, N=CH); 10.98 (s, 2H, 2NH exchangeable with D₂O). MS *m/z* (%): 280 (M⁺, 0.53); 238 (100.00). Anal. Calcd for C₁₀H₈N₄O₂S₂ (280.33): C, 42.85; H, 2.88; N, 19.99%. Found: C, 42.99; H, 2.90; N, 20.07%.

4.2. Antitumor activity

The *in-vitro* anti-tumor activity of the test compounds was performed in the Regional Center for Mycology and Biotechnology, Al Azhar University. The antiproliferative activities of the prepared compounds against colorectal cancer (Caco-2), hepatic cancer (HepG-2) and breast cancer (MCF-7) cell lines were evaluated using SRB method as described by Skehan et al., 1990^[38]. Exponentially growing cells were collected using 0.25% Trypsin-EDTA and seeded in 96-well plates at 1000-2000 cells/well in RPMI-1640 supplemented medium. After 24 hr, cells were incubated for 72 hr with various concentrations of the tested compounds. Following 72 hr treatment, the cells were fixed with 10% trichloroacetic acid for 1 h at 4 °C. Wells were stained for 10 min at room temperature with 0.4% SRB dissolved in 1% acetic acid. The plates were air dried for 24 h and the dye was solubilized with Tris-HCl for 5 min on a shaker at 1600 rpm. The optical density (OD) of each well was measured spectrophotometrically at 564 nm with an ELISA microplate reader (ChroMate-4300, FL, USA). The IC₅₀ values were calculated according to the equation for Boltzman sigmoidal concentration–response curve using the nonlinear regression fitting models (Graph Pad, Prism Version 5).

4.3. QSAR

As an initial step before working on the QSAR model fetching, the cytotoxic activity of the 24 compounds for breast cancer cell line (MCF-7) were presented as PIC₅₀ (-log (IC₅₀*10⁻⁶)). Next, the compounds were classified into two sets with ratio 3:1, training set including 18 compounds and test set including the other 6 compounds. To assure random classification and structural diversity, the test set includes at least one compound from each synthesis scheme. Many 2D

QSAR models have been built on the training set using Molecular Operating Environment (MOE 2016)^[32] with partial least squares (PLS) as model fitting procedure and examined on the test set compounds. The best one was chosen according to statistical values that assures the good prediction ability of the model internally and externally, as r^2 (correlation coefficient for training set of compounds) and pred_r^2 (predictive r^2 for the test set of compounds). The 2D descriptors were filtered using WEKA 3.9^[33-34] and contingency analysis in MOE^[32] to select the most relevant ones. Then, the resultant descriptors were tried by mix and match to form different models.

4.4. Pharmacophore

A ligand based pharmacophore model was built with regards to the MCF-7 breast cancer cell line cytotoxicity results using MOE 2016 based on flexible alignment of 15 structurally diverse compounds from the different synthesis schemes. The pharmacophore consensus threshold score was first set to 100% and there were no features available. Then, it was reduced to 97% which yielded only 3 feature and finally it was adjusted to 93% which resulted in 17 features. The best model was validated internally and externally.

4.5. In silico physicochemical and ADME properties prediction

The molecular structures were converted into SMILES database using MOE2016. Then, these SMILES were inserted as input in SwissADME website to calculate the physicochemical descriptors, pharmacokinetics properties, ADME parameters and medicinal chemistry friendliness.

Acknowledgement

The corresponding author would like to acknowledge ASRT for providing the funding grant ASRT-4/2016 part of which was used for partial support of this research work.

Conflict of Interest

The authors declare no conflict of interest.

References

- [1] J.J. Dimaggio, R.P. Warrell, J. Muindi, Y.-W. Stevens, S.J. Lee, D.A. Lowenthal, I. Haines, T.D. Walsh, L. Baltzer, S. Yaldae, C.W. Young, Phase I Clinical and Pharmacological Study of Merbarone, *Cancer Res.*, 1990, 50, 1151-1155.
- [2] J.M. Fortune, N. Osheroff, Merbarone Inhibits the Catalytic Activity of Human Topoisomerase II α by Blocking DNA Cleavage, *J. Biol. Chem.* 1998, 273, 17643-17650.
- [3] A.K. Larsen, A.E. Escargueil, A. Skladanowski, Catalytic topoisomerase II inhibitors in cancer therapy, *Pharmacol. Ther.*, 2003, 99, 167-181.
- [4] A. Ranise, A. Spallarossa, S. Schenone, O. Bruno, F. Bondavalli, A. Pani, M.E. Marongiu, V. Mascia, P. La Colla, R. Loddo, Synthesis and antiproliferative activity of basic thioanalogues of merbarone, *Bioorg. Med. Chem.*, 2003, 11, 2575-2589.
- [5] Y. Qin, L. Meng, C. Hu, W. Duan, Z. Zuo, L. Lin, X. Zhang, J. Ding, Gambogic acid inhibits the catalytic activity of human topoisomerase II α by binding to its ATPase domain, *Mol. Cancer Ther.*, 2007, 6, 2429-2440.
- [6] J. Schemies, W. Sippl, M. Jung, Histone deacetylase inhibitors that target tubulin, *Cancer Lett.* 2009, 280, 222-232.
- [7] Y. Cen, Sirtuins inhibitors: The approach to affinity and selectivity: a review, *Biochim. Biophys. Acta*, 2010, 1804, 1635-1644.
- [8] P. Sivaraman, S. Mattegunta, G.V. Subbaraju, C. Satyanarayana, B. Padmanabhan, Design of a novel nucleoside analog as potent inhibitor of the NAD dependent deacetylase, SIRT2, *Syst. Synth. Biol.*, 2011, 4, 257-263.
- [9] X. Kong, J. Qin, Z. Li, A. Vultur, L. Tong, E. Feng, G. Rajan, S. Liu, J. Lu, Z. Liang, M. Zheng, W. Zhu, H. Jiang, M. Herlyn, H. Liu, R. Marmorstein, C. Luo, Development of a novel class of B-Raf(V600E)-selective inhibitors through virtual screening and hierarchical hit optimization, *Org. Biomol. Chem.*, 2012, 10, 7402-7417.
- [10] S. Bruzzone, M.D. Parenti, A. Grozio, A. Ballestrero, I. Bauer, A. Del Rio, A. Nencioni, Rejuvenating sirtuins: the rise of a new family of cancer drug targets, *Curr. Pharm. Des.*, 2013, 19, 614-623.
- [11] N. R. Penthal, P. R. Ponugoti, V. Kasam, P. A. Crooks, 5-((1-Aroyl-1H-indol-3-yl)methylidene)-2-thioxodihydropyrimidine-4,6(1H,5H)-diones as potential anticancer agents with anti-inflammatory properties, *Bioorg. Med. Chem. Lett.*, 2013, 23, 1442-1446.
- [12] P. Bhatt, M. Kumar, A. Jha, Design, Synthesis and Anticancer Evaluation of Oxa/Thiadiazolyhydrazones of Barbituric and Thiobarbituric Acid: A Collective In Vitro and In Silico Approach, *Chemistry Select*, 2018, 3, 7060-7065.
- [13] S.R. Ramiseti, M.K. Pandey, S.Y. Lee, D. Karelia, S. Narayan, S. Amin, A. K. Sharma, Design and synthesis of novel thiobarbituric acid derivatives targeting both wild-type and BRAF-mutated melanoma cells, *Eur. J. Med. Chem.*, 2018, 143, 1919-1930.
- [14] J. Figueiredo, J. L. Serrano, E. Cavalheiro, L. Keurulainen, J. Yli-Kauhaluoma, V. M. Moreira, S. Ferreira, F.C. Domingues, S. Silvestre, P. Almeida, Trisubstituted barbiturates and thiobarbiturates: Synthesis and biological evaluation as xanthine oxidase inhibitors, antioxidants, antibacterial and anti-proliferative agents, *Eur. J. Med. Chem.*, 2018, 143, 829-842.
- [15] D.C. Young, T.R. Bailey, Methods for treating or preventing viral infections and associated diseases, US Patent 9920402, 2001.
- [16] S. Rajamaki, A. Innitzer, C. Falciani, C. Tintori, F. Christ, M. Witvrouw, Z. Debyser, S. Massa, M. Botta, Exploration of novel thiobarbituric acid-, rhodanine- and thiohydantoin-based HIV-1 integrase inhibitors, *Bioorg. Med. Chem. Lett.*, 2009, 19, 3615-3618.

- [17] J. H. Lee, S. Lee, M. Y. Park, H. J. Ha, H. Myung, Evaluation of inhibitory effects of thiobarbituric acid derivatives targeting HCV NS5B polymerase, *J. Microbiol. Biotechnol.*, 2010, 20, 510-512.
- [18] G. S. Hassan, N. A. Farag, G. H. Hegazy, R. K. Arafa, Design and Synthesis of Novel Benzopyran- 2- one Derivatives of Expected Antimicrobial Activity through DNA Gyrase- B Inhibition. *Arch. Pharm.*, 2008, 341, 725-733.
- [19] F. A. Ragab, T. A. A. Yahya, M. M. El-Naa, R. K. Arafa, Design, synthesis and structure–activity relationship of novel semi-synthetic flavonoids as antiproliferative agents, *Eur. J. Med. Chem.*, 2014, 82, 506-520.
- [20] M. A. Ismail, R. K. Arafa, M. M. Youssef, W. M. El-Sayed, Anticancer, antioxidant activities, and DNA affinity of novel monocationic bithiophenes and analogues, *Drug Des. Dev. Ther.*, 2014, 8, 1659-1672.
- [21] N. E. Abo-Elmagd, R. F. George, M. A. Ezzat, R. K. Arafa, New 1-phthalazinone scaffold based compounds: Design, synthesis, cytotoxicity and protein kinase inhibition activity, *Mini-Rev. Med. Chem.*, 2018, 18, 1759 - 1774.
- [22] U. Pindur, N,N-Dimethylformamide Diethyl Acetal, e-EROS (2001).
- [23] F. A. Abu-Shanab, S. A. S. Mousa, E. A. Eshak, A. Z. Sayed, A. Al-Harrasi, Dimethylformamide Dimethyl Acetal (DMFDMA) in Heterocyclic Synthesis: Synthesis of Polysubstituted Pyridines, Pyrimidines, Pyridazine and Their Fused Derivatives, *Int. J. Org. Chem.*, 2011, 1, 207-214.
- [24] D. Kumar, V. Judge, R. Narang, S. Sangwan, E. De Clercq, J. Balzarini, B. Narasimhan, Benzylidene/2-chlorobenzylidene hydrazides: synthesis, antimicrobial activity, QSAR studies and antiviral evaluation, *Eur. J. Med. Chem.*, 2010, 45, 2806-2816.
- [25] M. I. El-Zahar, S. S. Abd El-Karim, M. E. Haiba, Synthesis and Cytotoxic Evaluation of Some Novel 6-(Benzofuran-2-yl)-4-(4-Fluorophenyl)Pyridines, *World J. Chemistry*, 2009, 4, 182-194
- [26] M. M. Abd El-All, A. H. Halawa, A. A. Hassan, M. A. El-Nassag, G. A. Abd El-Jaleel, E. M. Eliwa, A. H. Bedair, Synthesis and Antioxidant Activity of Some Derivatives of 2-(2-oxo-4-phenyl-2h-chromen-7-yloxy)AcetoHydrazide, *J. Atoms Mol.*, 2013, 3, 537-552.
- [27] W.S. El-Hamouly, K. M. Amin, S. A. El-Assaly, E. A. Abd El-Meguid, Synthesis and antitumor activity of some new N-substituted-sulfonyl, 1,2,4-triazole, N-substituted-benzylidene and pyrrole derivatives attached to 4-(benzo[d]thiazol-2-yl)benzohydrazide, *Der pharma chem.*, 2011, 3, 293-306.
- [28] A. H. Sharba, R. H. Al-Bayati, M. Aouad, N. Rezki, Synthesis of oxadiazoles, thiadiazoles and triazoles derived from benzo[b]thiophene, *Molecules*, 2005, 10, 1161-1168.
- [29] P. Kumar, B. Narasimhan, D. Sharma, Substituted benzoic acid benzylidene/furan-2-yl-methylidene hydrazides: synthesis, antimicrobial evaluation and QSAR analysis, *Arkivoc*, 2008, 13, 159-178.
- [30] L. Srikanth, U. Naik, R. Jadhav, N. Raghunandan, J. V. Rao, Synthesis and Evaluation of New Phenylaminothiadiazolo-Oxadiazolo-1,3benzoxazoles for Their Antibacterial Activity, *Int. J. Pharm. Biol. Sci.* 2010, 1, 260-271.
- [31] H. A. Abdel-Aziz, T. Elsaman, M.I. Attia, A. M. Alanazi, The reaction of ethyl 2-oxo-2H-chromene-3-carboxylate with hydrazine hydrate, *Molecules*, 2013, 18, 2084-2095.
- [32] Molecular Operating Environment (MOE), 2016.08; Chemical Computing Group Inc., 1010 Sherbrooke St. West, Suite #910, Montreal, QC, Canada, H3A 2R7, 2016.
- [33] M. Hall, E. Frank, G. Holmes, B. Pfahringer, P. Reutemann, I. H. Witten, The WEKA data mining software: an update. *ACM SIGKDD explorations newsletter*, 2009, 11, 10-18.

- [34] E. Frank, M. A. Hall, I. H. Witten (2016). The WEKA Workbench. Online Appendix for "Data Mining: Practical Machine Learning Tools and Techniques", Morgan Kaufmann, Fourth Edition.
- [35] RNA Targeted Library <http://www.otavachemicals.com/products/targeted-libraries-and-focused-libraries/rna-binding> (last accessed Oct 24, 2018).
- [36] SwissADME: a free web tool to evaluate pharmacokinetics, drug-likeness and medicinal chemistry friendliness of small molecules. *Sci. Rep.*, 2017, 7, 42717.
- [37] S. J. Capuzzi, E. N. Muratov, A. Tropsha, Phantom PAINS: Problems with the Utility of Alerts for Pan-Assay Interference CompoundS, *J. Chem. Inf. Model.*, 2017, 57, 417–427.
- [38] P. Skehan, R. Storeng, D. Scudiero, A. Monks, J. McMahon, D. Vistica, J. T. Warren, H. Bokesch, S. Kenney, M. R. Boyd, New colorimetric cytotoxicity assay for anticancer-drug screening. *J. Natl. Cancer Inst.*, 1990, 82, 1107-1112.

Legends

List of figures:

- Figure 1:** Merbarone I and thiobarbiturate analogues with promising anticancer activity.
- Figure 2:** Structural design of the target thiobarbiturate derivatives. Fragment replacement profile of reported thiobarbiturates (**V**, **VI**) and designed thiobarbituric acid derivatives as antitumor. First modification (upper panel) in compounds **2**, **3a-h**, **7**, **10a-c**, **11** and **12a-d**, moiety *B* was replaced by different amines e.g. amino group, hydrazone, hydrazinocarbonyl, hydrazinosulfone and thiosemicarbazide moieties. Second modification in compounds **8a-c** (middle panel) explored isosteric replacement of furan ring by pyrazole moiety. Third modification (lower panel) for compounds **4-6** and **9** included replacing moiety *B* in **V** and **VI** with aliphatic/aryl diamine linker to obtain bis-thiobarbiturates.
- Figure 3:** Correlation plot of the training set showing R^2 value = 0.755
- Figure 4:** Correlation plot of the test set showing R^2 value = 0.704
- Figure 5:** Five features of the pharmacophore model on the 15 aligned compounds
- Figure 6:** 3D spatial distribution of the five pharmacophoric features

List of tables:

- Table 1:** IC_{50} of the test set of compounds against human colorectal cancer (Caco-2), hepatic cancer (HepG-2), and breast cancer (MCF-7).
- Table 2:** Compounds in the training set with their pIC_{50} values (MCF-7 cell line), predicted pIC_{50} , residuals and Z-scores
- Table 3:** Compounds in the test set with their pIC_{50} values (MCF-7 cell line), predicted pIC_{50} and the residual values.
- Table 4:** Drug-likeness based on Lipinski's rule of five, TPSA and number of rotatable bonds
- Table 5:** Pharmacokinetics and medicinal chemistry parameters

List of schemes:

- Scheme 1:** Synthesis of derivatives **3a-h**.
- Scheme 2:** Synthesis of derivatives **4-6**.
- Scheme 3:** Synthesis of derivatives **7** and **8a-c**.
- Scheme 4:** Synthesis of derivative **9**.
- Scheme 5:** Synthesis of derivatives **10a-c**, **11** and **12a-d**.

List of abbreviations:

- PEOE:** Partial Equalization of Orbital Electronegativities [Gasteiger 1980]
- VSA:** Van der Waals surface area
- BCUT:** Burden cas university of texas descriptors using adjacency matrix
- SMR:** Molecular refractivity
- FNEG:** Fractional Negative
- QSAR:** Quantitative structure activity relationship
- XRMSE:** Cross root mean square error
- TPSA:** Total polar surface area
- Mw:** Molecular weight
- 2D:** Two dimensional
- PiR:** Pi ring center

Aro:	Aromatic
Hyd:	Hydrophobic
Acc:	H-bond acceptor
Don:	H-bond donor
IR:	Infrared spectroscopy
MS:	Mass spectrometer
NMR:	Nuclear magnetic resonance

ACCEPTED MANUSCRIPT

Graphical Abstract

